REPORT NO. 81
JULY, 1954.

THE COLLEGE OF AERONAUTICS

CRANFIELD

Note on the Results of Some Profile Drag Calculations for a Particular Body of Revolution at Supersonic Speeds

-by-

J.R. Wedderspoon, B.Sc., D.C.Ae.,
and
A.D. Young, M.A., F.R.Ae.S.
of the Department of Aerodynamics

SUMMARY

Details additional to those discussed in College of Aeronautics Report No. 73 are given of the method developed for the calculation of the profile drag of bodies of revolution at supersonic speeds and zero incidence. The method has been applied to a particular body of fineness ratio 7.5 (see Fig. 1) for Mach numbers ranging from 1.5 to 5.0, Reynolds numbers ranging from 10^6 to 10^8 and transition positions ranging from the nose to the tail end of the body. The calculations assume zero heat transfer. The results indicate that the overall difference in profile drag between fully laminar and fully turbulent flow decreases rapidly with mainstream Mach number and rather more rapidly than does the corresponding difference for a flat plate, and at Mach numbers greater than about 2 the profile drag of the body with fully turbulent flow is less than that of a flat plate (Fig. 14).

However, the effects of rotation in the flow introduced by the nose shock and secondary effects on the development of the boundary layer caused by the modification of the external pressure distribution due to the boundary layer have not been taken into account in the main body of calculations and it appears that they may appreciably alter the calculated profile drag values for the high end of the Mach number range considered bringing the value for the body with fully turbulent flow nearer the flat plate value. A further comprehensive series of calculations covering a range of fineness ratios is planned in which allowance for these factors will be made.

MAIN NOTATION

b	radius of base of body
c_{f_o}	local frictional stress coefficient in terms of undisturbed stream values of velocity and density
c_{f_n}	local frictional stress coefficient in terms of density and velocity just aft of nose shock $(2\tau_w/\rho_n u_n^2)$
C_F	overall skin friction coefficient (based on surface area of body)
C_{D_p}	form drag coefficient (based on surface area of body)
C_{D_o}	profile drag coefficient $(C_F + C_{D_p})$
C_{p_o}	pressure coefficient $\left[(p-p_o)/p_o\right]$
C_{p_b}	pressure coefficient for aft body $\left[(p-p_b)/p_b\right]$
D	maximum diameter of body
$F(x), G(x)$	functions defined in equation (9) (see also Ref. 1)
f, g	function defined in equation (2) (see also Ref. 8)
$h(M_1, R_o)$	function given in Ref. 1 (Fig. 2)
H	ratio of displacement thickness to momentum thickness of boundary layer (δ^*/θ)
K	hypersonic similarity parameter $(M_o D/L)$
L	linear dimension used in K, e.g. length of head (L_H) or aft body (L_B)
M	Mach number
l	overall length of body

p	pressure
p_b	pressure just in front of aft body
r_o	radius of cross section of body
R	Reynolds number
s	distance measured along meridian profile from nose/l
S	surface area of body/l^2
t	see Fig. 1(d)
u	velocity component parallel to surface of body
x	axial distance measured from nose/l
y	distance measured normal to meridian profile/l
x_H	non-dimensional axial distance for head, i.e. xl/L_H
x_B	axial distance for aft body measured from beginning of aft body/L_B
γ	ratio of specific heats, assumed equal to 1.4
ε	effective increase of cross sectional radius due to boundary layer
δ	boundary layer thickness
θ	momentum thickness of boundary layer (see equation 3)
δ^*	displacement thickness of boundary layer (see Ref. 1)
Λ	generalised Pohlhausen parameter (see equation 4)
μ	coefficient of viscosity
ω	exponent in temperature viscosity relation
σ	Prandtl number
$\bar{\psi}$	angle between tangent to meridian profile and axis
λ, ψ	angles required for equivalent ogive of curvature method (Ref. 7), see equation 14.

suffix	o	refers to undisturbed stream values
suffix	1	refers to local values just outside the boundary layer
suffix	n	refers to values at nose just aft of nose shock
suffix	w	refers to values at the surface
suffix	H	relates to the forebody or head
suffix	B	relates to the boat-tail aft body
suffix	L	relates to laminar flow
suffix	T	relates to turbulent flow
suffix	ε	relates to the effective shape allowing for displacement due to the boundary layer.

1. Introduction

In College of Aeronautics Report No. 73[1] the analysis was developed for calculating the profile drag of aerofoils and bodies of revolution at supersonic speeds. This present paper is concerned with the details of the application of that analysis to bodies of revolution of the type illustrated in Fig. 1 having circular arc ogival heads, cylindrical centre sections and parabolic boat tailed aft-bodies, and the results obtained for one body of fineness ratio 7.5 whose geometry is given in more detail in the Appendix. These calculations cover free stream Mach numbers of 1.5, 2.5 and 5.0, Reynolds numbers of 10^6, 10^7, and 10^8 and with transition positions at 0, $\frac{2}{3}\,l$ and l from the nose where l is the overall body length. A later paper will give the results of comprehensive calculations covering a range of fineness ratios.

The term profile drag is here used (as in Report No. 73) to denote the drag that arises from the viscosity of the medium, and is thus the sum of the skin friction drag and the change in the wave drag due to the presence of the boundary layer. This latter contribution to the profile drag is referred to as the form drag. The analysis therefore involves the determination of the development of the boundary layer in the laminar and turbulent states, and the associated change in pressure distribution from that given by inviscid flow theory due to the effective displacement of the body surface arising from the presence of the boundary layer.

The following assumptions are made:-

(i) The heat transfer is zero.

(ii) There is no separation of the boundary layer from the body.

(iii) The value of the Prandtl number (σ) is taken to be 0.72.

(iv) The value of γ is taken to be 1.40.

(v) The value of the exponent (ω) of the viscosity - temperature relation ($\mu = \text{const.}\ T^{\omega}$) is 8/9.

2. Details of the method of analysis

2.1. Pressure distribution

Before the development of the boundary layer can be followed the pressure distribution on the body must be determined, in the first instance for inviscid flow.

Since it is ultimately intended to consider a number of bodies of different fineness ratio it is convenient to make use of the hypersonic similarity law.[2,3] This law states that subject to certain limitations of fineness ratio and Mach number similarly shaped bodies of revolution at zero incidence have the same non-dimensional pressure distributions at the same value of the parameter $K = M_o D/L$, where M_o is the undisturbed stream Mach number, D is the maximum body diameter and L is the body length which might in this context be that of the head or boat tail alone (i.e. L_H or L_B). Curves of the pressure coefficient against K for various positions downstream from the nose were therefore constructed.

To obtain the pressure distributions over the forebody the data from Ref. 3 were used. The relevant curves are reproduced in Fig. 2 where K_H is the hypersonic parameter with the head length L_H as reference body length and $C_{p_o} = (p-p_o)/p_o$.

For the centre section the data of Ref. 3 for a cylinder following an ogival head were plausibly extended and are shown in Fig. 3 in the form used for these calculations.

For the boat tailed aft-body the results of the calculations by Fraenkel[4] were used, supplemented for other values of K_B by calculations using Van Dyke's second order theory.[5] The symbol K_B here denotes the hypersonic parameter with the tail length as reference body length. It should be noted that for such calculations the conditions at the end of the centre section are assumed to be the same as the free stream conditions. Consequently, the non-dimensional pressures are given in the form of $C_{p_b} = (p-p_b)/p_b$, where p_b is the pressure immediately ahead of the aft-body. The results of the calculations are shown in Fig. 4.

It was initially hoped that with a Mach number range of 1.5 to 5.0 the pressure distribution for any overall fineness ratio between about 7.5 and 11 could be found with acceptable accuracy for the purpose of profile drag estimation from Fig. 2, 3 and 4. However, the effects of rotation in the flow introduced at the nose shock have not been included in the calculations of Ref. 3 on which Fig. 2 and 3 are based. Subsequent to the completion of much of the work described in this paper the attention of the authors was drawn to Ref. 6 in which allowance for rotation effects is made and it is clear that these effects can be appreciable for values of $K_H > 1.0$ and therefore for the body considered at Mach numbers greater than 2.5. For the purpose of profile drag estimation their significance will be clearly less than for the estimation of wave drag, nevertheless it is intended to investigate this point and subsequent calculations that are planned will be made with allowance for rotation effects on the pressure distribution.

2.2. The laminar boundary layer

From Ref. 1 (equation 33) we have that the laminar boundary layer momentum thickness, θ, at any station s_1 can be obtained from the formula

$$\left[\rho_1 r_o^2 \theta^2\right]_{s_1} = \frac{4}{R_n . f . u_1^g} \int_o^{s_1} \rho_1 u_1^{g-1} r_o^2 . ds \quad , \quad \ldots\ldots(1)$$

where ρ_1 and u_1 are the velocity and density just outside the boundary layer, respectively, made non-dimensional in terms of the corresponding quantities (ρ_n, u_n) just aft of the nose shock at the nose of the body. The Reynolds number R_n is similarly defined by

$$R_n = \frac{u_n \, l \, \rho_n}{\mu_n} \quad ,$$

where l is the overall length of the body.
The distance s is measured along a meridian profile of the body and is made non-dimensional by dividing by l. The functions f and g are given by

$$\left.\begin{aligned} f &= 9.072 \left[1 + 0.365(\gamma-1)\, M_n^2\right]^{1-\omega} \\ g &= 9.18 + 1.436\, M_n^2 - \frac{f}{3}\left[1 + \frac{(\gamma-1)}{2}\,\sigma^{\frac{1}{2}}\, M_n^2\right]^{\omega} \end{aligned}\right\} \quad (2)$$

where M_n is the Mach number just aft of the nose shock at the nose of the body.

The momentum thickness θ is defined by

$$\theta = \int_o^{\delta} \frac{\rho u}{\rho_1 u_1}\left(1 + \frac{y}{r_o}\cdot \mathrm{Cos}\,\bar{\psi}\right)\left(1 - \frac{u}{u_1}\right)\cdot dy \quad ..(3)$$

where y is measured normal to the body surface, δ is the boundary layer thickness, r_o is the radius of cross-section of the body, and $\bar{\psi}$ is the angle between the tangent to the meridian of the body and the axis. All distances are made non-dimensional in terms of the body length l.

The relation between s and the non-dimensional axial distance, x, is given by

$$s = \int_o^{x} \left[1 + \left(\frac{dr_o}{dx}\right)^2\right]^{\frac{1}{2}} \cdot dx \,.$$

Given the shape of the body and the pressure distribution the quantities ρ_1 and u_1 as functions of s(or x) can be readily evaluated on the assumption of isentropic flow outside the boundary layer aft of the nose shock. Hence from equation (1) the distribution of θ along the body can be determined.

The skin friction distribution can then be obtained from (equation 34, Ref. 1)

$$\left.\begin{aligned} c_{f_n} &= \frac{2\tau_w}{\rho_n u_n^2} = \frac{(\Lambda + 12)u_1}{3\, R_n \cdot f \cdot \theta} \\ &\text{where } \tau_w \text{ is the frictional stress, and} \\ \Lambda &= R_n\left[\frac{du_1}{ds}\cdot \theta^2 f^2 \rho_1 \mu_w\right]. \end{aligned}\right\} \quad \ldots\ldots(4)$$

The wall value of the viscosity, μ_w, is given, with the assumptions made, by the formula

$$\mu_w = \left\{1 + \frac{(\gamma-1)}{2}\, M_n^2\left[1 + u_1^2\,(\sigma^{\frac{1}{2}} - 1)\right]\right\}^{\omega} \quad \ldots\ldots\ldots(5)$$

The contribution of the skin friction in the laminar boundary layer to the overall skin friction coefficient is then

$$C_{F_L} = \left[\frac{2\pi}{S} \int_o^{x_T} c_{f_n} . r_o \, dx \right] . \frac{\rho_n u_n^2}{\rho_o u_o^2} \qquad \text{.....(6)}$$

where $S.l^2$ is the surface area of the body, and suffix o relates to quantities in the undisturbed stream and suffix T to the transition point.

From the derived distribution of θ the distribution of the displacement thickness can be obtained using the relations

$$\left.\begin{aligned} \delta^{**} &= H.\theta \\ \text{where} \quad H &= 2.59 \left(1 + 0.277\, M_n^2\right) . \end{aligned}\right\} \qquad \text{.....(7)}$$

2.3. The turbulent boundary layer

From equation (36) of Ref. 1, and taking the recommended values of n and C_2 (6 and 0.00878, respectively) for the range of Reynolds number considered we have

$$(r_o\theta)^{\frac{6}{5}} = \frac{0.010536\, R_n^{-1/5} \left[\int_{x_T}^{x} G(x) r_o^{6/5} \exp\left[\int_{x_T}^{x} \frac{6}{5} F(x) \frac{ds}{dx} . dx \right] + (r_o\theta)_T^{6/5} \right]}{\left[\exp \int_{x_T}^{x} \frac{6}{5} F(x) \frac{ds}{dx} . dx \right]} \qquad \text{.....(8)}$$

and the skin friction coefficient is given by (equation 37, Ref. 1)

$$\left.\begin{aligned} c_{f_n} &= 0.01756\, R_n^{-1/5} \rho_1 u_1^2 \, G(x) \, \theta^{-1/5} , \\ \text{where} \quad F(x) &= \frac{du_1}{ds} . \frac{1}{u_1} \left[(H+2) - M_1^2 \right] \\ G(x) &= \left(\frac{u_1}{\nu_1} \right)^{-1/5} . h(M_1, R_o) \end{aligned}\right\} \qquad \text{.....(9)}$$

and the functions $h(M_1, R_o)$ and H are given in Fig. 2 and 3 of Ref. 1.

From the distribution of θ the distribution of the displacement thickness δ^* is readily obtained from the relation

$$\delta^* = H.\theta.$$

The contribution of the skin friction in the turbulent boundary layer to the overall skin friction coefficient is

$$C_{F_T} = \left[\frac{2\pi}{S}\int_{x_T}^{1} c_{f_n}.r_o.dx\right] \frac{\rho_n.u_n^2}{\rho_o\, u_1^2} \qquad \ldots\ldots\ldots\ldots(10)$$

2.3. The form drag

It is shown in Ref. 1 that the effect of the boundary layer on the external flow can be taken as equivalent to that of displacing the surface outwards through a distance ε normal to itself where ε is related to the displacement thickness δ^* by the equation[x]

$$\delta^* = \varepsilon + \frac{\varepsilon^2}{2r_o} . \qquad \ldots\ldots\ldots\ldots(11)$$

We therefore require to develop a method of acceptable accuracy for calculating the change in the external pressure distribution due to this displacement of the surface which may be assumed to be small except perhaps over the tail.

The method adopted is as follows. Consider the head first; if we were to apply the 'equivalent ogive of curvature' method of Bolton-Shaw and Zienkiewicz[7] to the displaced shape, which we will denote by suffix ε, then at each point we would require to determine the equivalent hypersonic parameter, K_{H_ε}, and the equivalent distance downstream from the nose $x_{H_\varepsilon}.L_\varepsilon$ by means of the formulae (see Ref. 7)

$$K_{H_\varepsilon} = 2\, M_o \tan\frac{\chi\varepsilon}{2} \qquad \ldots\ldots\ldots\ldots(12)$$

/and ...

---

x The distance ε is here non-dimensional in terms of the overall body length l.

and

$$x_{H_\varepsilon} = \left(1 - \frac{\sin \vartheta_\varepsilon}{\sin \chi_\varepsilon}\right) . \qquad \text{.....(13)}$$

The angles χ_ε and ϑ_ε are defined in terms of the ordinate r_{o_ε}, and its derivatives with respect to x by the formulae

$$\chi_\varepsilon = \cos^{-1} \left\{ \frac{1 + r'^2_{o\varepsilon} + r_{o\varepsilon} . r''_{o\varepsilon}}{(1 + r'^2_{o_\varepsilon})} \right\}$$

and $\qquad \text{.....(14)}$

$$\vartheta_\varepsilon = \tan^{-1} r'_{o_\varepsilon} = \tan^{-1} \left(r'_o + \frac{d\varepsilon}{dx}\right) .$$

We then write

$$\Delta K_H = K_{H_\varepsilon} - K_H$$

and $\qquad \Delta x_H = x_{H_\varepsilon} - x_H ,$

and assuming that the corresponding pressure change is small we have

$$\Delta C_{p_o} = \left(\frac{\partial C_{po}}{\partial K_H}\right) . \Delta K_H + \left(\frac{\partial C_{po}}{\partial x_H}\right) . \Delta x_H , \qquad \text{.....(15)}$$

where the quantities $\left(\frac{\partial C_{po}}{\partial K_H}\right)$ and $\left(\frac{\partial C_{po}}{\partial x_H}\right)$ are determined from the curves of Fig. 2.

The form drag contribution of the head is then given by

$$\left(\Delta C_{D_p}\right)_H = \frac{4\pi}{\gamma S M_o^2} \int_o^{L_H/l} \Delta C_{p_o} . \frac{dr_o}{dx} . r_o . dx \qquad \text{.....(16)}$$

For the form drag contribution of the aft-body a similar though somewhat more complicated method is used. It was assumed that the displaced profile is parabolic in form like the actual profile finishing with a base radius of cross-section equal to 5/9 the maximum radius of cross-section. Since the displacement ε will grow more rapidly over the forward portion of the tail than r_o decreases $d(r_o+\varepsilon)/dx$ is zero at some point

$x_{\varepsilon 1}$ downstream of the beginning of the tail (see Fig. 1d). The displaced tail must therefore be assumed to begin at this point. Writing L_{B_ε} for the effective length of the displaced tail, D_ε for its maximum diameter and t for the length of the actual tail minus $x_{\varepsilon 1}$ (all lengths being made non-dimensional in terms of l the overall length of the body) then we have from the assumed parabolic formula for its profile (see the Appendix) that

$$L_{B\varepsilon}^2 = \frac{4\, t^2\, D_\varepsilon}{9(D_\varepsilon - 2b_\varepsilon)} \qquad \text{.....(17)}$$

where b_ε is the radius of cross-section of the displaced profile in the plane of the base of the actual profile. It follows that having determined D_ε, b_ε and $x_{\varepsilon 1}$ and therefore t we can calculate $L_{B\varepsilon}$. The corresponding hypersonic parameter is then given by

$$K_{B\varepsilon} = M_\varepsilon \Big/ \frac{L_{B\varepsilon}}{D_\varepsilon} \quad , \qquad \text{.....(18)}$$

where M_ε is Mach number of the flow just outside the boundary layer at the point $x_{\varepsilon 1}$, whilst the corresponding fractional distance downstream from the beginning of the effective tail is

$$x_{B\varepsilon} = (x_B L_B - x_{\varepsilon 1})/L_{B\varepsilon} \, . \qquad \text{.....(19)}$$

Writing

$$\Delta K_B = K_{B\varepsilon} - K_B$$

and

$$\Delta x_B = x_{B\varepsilon} - x_B$$

we have

$$\Delta C_{p_b} = \left(\frac{\partial C_{p_b}}{\partial K_B}\right) \Delta K_B + \left(\frac{\partial C_{p_b}}{\partial x_T}\right) \Delta x_B \qquad \text{.....(20)}$$

but we here note that

$$\Delta C_{p_b} = \frac{p_\varepsilon - p_{b\varepsilon}}{p_{b\varepsilon}} - \frac{p - p_b}{p_b} \qquad \text{.....(21)}$$

where $p_{b\varepsilon}$ is the pressure at $x_{\varepsilon 1}$.
Hence, it follows that the change in pressure due to the displacement

downstream of $x_{\varepsilon 1}$ is

$$\Delta p = p_\varepsilon - p = p\left[\frac{p_{b\varepsilon}}{p_b} - 1\right] + p_{b\varepsilon} \cdot \Delta C_{p_b} \cdot \quad \ldots\ldots(22)$$

The effect of the displacement on the pressure from just aft of the head to the point $x_{\varepsilon 1}$ may with reasonable accuracy be obtained on the assumption that it is the same as that in a simple wave flow i.e.

$$p_\varepsilon - p = \Delta p = \frac{\gamma p M_1^2}{\sqrt{M_1^2 - 1}} \cdot \frac{d\varepsilon}{ds} \quad \ldots\ldots\ldots\ldots(23)$$

and in particular this formula enables us to determine the pressure $p_{b\varepsilon}$ at the point $x_{\varepsilon 1}$ for substitution in equation (22). The contribution of the aft-body to the form drag coefficient is finally

$$\left(\Delta C_{D_p}\right)_B = \frac{4\pi}{\gamma S M_o^2} \int_{l_B}^{l} \frac{\Delta p}{p_o} \cdot \frac{dr_o}{dx} \cdot r_o \cdot dx \quad \ldots\ldots\ldots(24)$$

where l_B is the distance from the nose of the body to the beginning of the tail made non-dimensional in terms of the body length l.

The total form drag coefficient is then

$$C_{D_p} = \left(\Delta C_{D_p}\right)_H + \left(\Delta C_{D_p}\right)_B \cdot \quad \ldots\ldots\ldots\ldots(25)$$

It will be appreciated that if the calculated change of pressure over the body due to the boundary layer is large then the calculations of the boundary layer development should be repeated with the modified pressure distribution leading to a new value of the form drag and so on, until successive calculated changes in the pressure distribution due to the boundary layer produce negligible changes in the form drag.

3. Results and Discussion

3.1. Mach number and pressure distribution

Fig. 5 shows the calculated inviscid flow distribution of Mach number over the body considered for main stream Mach

numbers of 1.5, 2.5 and 5.0. It will be noted that in all cases the local Mach number was somewhat higher than the main stream value over the centre-body and aft-body.

The corresponding calculated pressure distributions are shown in Fig. 6. The rapid increase in the magnitude of the negative pressure gradient over the head with increase of main stream Mach number is noteworthy.

3.2. Skin friction results

The overall skin friction results are shown plotted in different ways in Fig. 8, 9 and 10 treating main stream Mach number, transition position and Reynolds number as independent variables and the results are also given in Table I. Perhaps the most striking feature of these results is the fact that the difference between the calculated values of skin friction for fully laminar and fully turbulent flow decreases rapidly with increase of Mach number and decrease of Reynolds number and is almost negligible in the case $M_o = 5$, $R_o = 10^6$. In Fig. 11 the results for $R_o = 10^6$, 10^7 and 10^8 are compared with the corresponding results for a flat plate and it will be seen that whilst the difference in the skin friction for fully laminar and fully turbulent flow also decreases markedly for the flat plate the decrease is not quite so great as for the body. Indeed the skin friction drag of the body with fully turbulent flow is less than that of the flat plate for Mach numbers greater than about 2.

Fig. 7 shows the distributions of skin friction over the body in the cases of fully laminar and fully turbulent flow at a Reynolds number of 10^6 and for $M_o = 1.5$, 2.5 and 5.0 and it will be seen that whereas in the fully laminar case the skin friction over the head shows a marked increase with M_o with a small decrease over the centre-body and aft-body, in the fully turbulent case there is a marked decrease in skin friction with increase of M_o over almost all the body except the forward half of the head.

It appears that the increase in skin friction with M_o over the head in the laminar case results largely from the greater importance that the positive velocity gradient there plays in the

laminar than in the turbulent case.* Further, it is a consequence of the large velocity gradient over the nose that the laminar skin friction coefficient of the body is somewhat higher than that of a flat plate. The cause of the very marked fall of the skin friction over the major part of the body with increase of M_o with fully turbulent boundary layer is rather more difficult to assess closely. An appreciable fall may be expected since it is inherent in the basic flat plate results on which the calculations are founded but we see from Fig. 7 that the calculated reduction is considerably greater than that for a flat plate. Referring to Fig. 6 we see that over much of the body the local Mach number is somewhat higher than the main stream value and so we may expect the flat plate reduction of skin friction with M_o to be somewhat magnified. Further the local values of $\rho_1 u_1^2$ (to which the local skin friction coefficient is proportional) falls with increase of M_1 in the range of Mach numbers covered. We might therefore expect the skin friction in the turbulent case for the body to decrease with Mach number somewhat more rapidly than on a flat plate but the actual rate of decrease is nevertheless surprisingly high. However, relevant to this point are the corrections that will need to be made in the extreme cases of high Mach number and low Reynolds number for secondary effects of the boundary layer on the pressure distribution reacting back on the boundary layer development and also for the effects of rotation. The possible effects of these corrections are discussed in §3.5 where it is concluded that they may appreciably modify the picture at high Mach numbers bringing the body and flat plate skin friction values for fully turbulent flow into closer agreement.

3.3. Form drag results

The results of the form drag calculations are shown in Fig. 12 and Fig. 13 illustrates a 'carpet' plot for the case $M_o = 5$. The results are also given in Table II.

The general variations of form drag with transition position and Reynolds number are as described in Ref. 1 but the overall increase with M_o is at first sight surprising. This

/appears ...

* In the momentum equation the term du_1/ds is multiplied by $(H+2-M_1^2)$ and H for the laminar boundary layer is almost twice as great as H for the turbulent boundary layer at any given Mach number.

appears to be related to the fact that whereas the boundary layer causes an increment in pressure over the head which increases fairly rapidly with Mach number in the range covered, the corresponding pressure increment over the tail increases far less rapidly with Mach number. The reason for this can be seen from Fig. 2 and 4 where it will be noted that the quantities $(\partial C_{p_o}/\partial K_H)$ and $(\partial C_{p_o}/\partial x_H)$ for the head are considerably greater than the corresponding quantities $(\partial C_{p_b}/\partial K_B)$ and $(\partial C_{p_b}/\partial x_B)$ for the tail. Changes of Mach number result most directly in changes of the hypersonic parameters K_H and K_B and also in some changes in the position parameters x_H and x_B, and the net effect is that the positive form drag contribution of the head increases more rapidly with Mach number than does the negative form drag contribution of the tail.

3.4. Profile drag results

The profile drag coefficients for the cases considered are shown in Fig. 14 and are also given in Table III. The corresponding curves for fully laminar and fully turbulent flow over a flat plate are shown in Fig. 14 for comparison. The general trend of the results is very much the same as for the skin friction coefficient results showing in particular the relatively small effect of transition position at a Mach number of 5.0 and Reynolds number of 10^6. The contribution of the form drag is in general small although in the extreme case of fully laminar or fully turbulent flow at $M_o = 5$ it can be of the order of 10 - 15 per cent of the profile drag.

3.5. Secondary effects and the effects of rotation

It is clear that where the calculated displacement ε of the profile is not small compared with the radius of cross-section further iterative calculations may be necessary to ensure that the calculated development of the boundary layer is sufficiently consistent with the finally determined pressure distribution.

In the case of the fully turbulent boundary layer, $M_o = 5$, and $R_o = 10^6$ the calculated value of the ratio ε/r_o at the end of the body was indeed of the order of unity, although in all other

cases it was considerably smaller. This case was therefore used as a test case to assess the effect of a second approximation. The skin friction distribution was therefore recalculated using the pressure distribution as given at the end of the first stage of allowing for boundary layer effects. The results are shown in Fig. 15 and it will be seen that the change in skin friction in going from the first to the second stage is by no means insignificant and it results in an overall increase of the skin friction coefficient of about 10 per cent. This effect would therefore increase somewhat the small difference given by the first stage between the profile drag with fully laminar and with fully turbulent boundary layers at high Mach numbers and low Reynolds numbers although it would not alter the general trend of a marked reduction of this case inherent in the flat plate data which are basic to these calculations.

However, as we have already noted, at the highest Mach numbers for this body the effect of rotation which has been ignored for these calculations would also make an appreciable effect on the pressure distribution causing in general an overall rise in pressure. This would therefore have a similar effect on the calculated skin friction as the change in pressure due to the presence of the boundary layer and the effects may well be of comparable magnitude. We may in consequence expect that when full allowance is made for these corrections the fully turbulent profile drag values for the body will be much closer the flat plate value at the Mach number of 5.0 than is indicated in Fig. 14. Nevertheless it is likely to be smaller than the flat plate value, a possibility which is in interesting contrast to subsonic results.

In the further and more comprehensive calculations which are contemplated for a range of fineness ratios it is intended to make proper allowance for both secondary effects and the effects of rotation.

4. Conclusions

The calculations of profile drag for the particular body considered indicate that the overall difference in profile drag between fully laminar and fully turbulent flow decreases rapidly with main stream Mach number and rather more rapidly than does the

corresponding difference for a flat plate. Indeed at Mach numbers greater than about 2 the profile drag of the body with fully turbulent flow is less than that of the flat plate. If this is confirmed by more comprehensive calculations as a general result it will be of significance in assessing the value of striving for large extents of laminar flow at high Mach numbers. However, the effects of rotation in the flow introduced by the nose shock and secondary effects on the boundary layer development due to the modification of the external pressure distribution caused by the boundary layer are of appreciable significance at the highest Mach number considered ($M_o = 5$) and it is likely that when allowance is made for these effects that the drag coefficient of the body for fully turbulent flow will be much closer to that of the flat plate than is indicated by these calculations (Fig. 14). A further comprehensive series of calculations covering a range of fineness ratios is planned in which allowance will be made for these factors.

REFERENCES

No.	Author	Title
1.	Young, A.D.	The calculation of the profile drag of aerofoils and bodies of revolution at supersonic speeds. College of Aeronautics Report No. 73 (1952)
2.	Tsien, H.	Similarity laws of hypersonic flows. J. Maths. and Physics Vol.25, No.3, Oct. 1946.
3.	Ehret, D.M., Rossow, V.J., Stevens, V.I.	An analysis of the applicability of the hypersonic similarity law to the study of flow about bodies of revolution at zero angle of attack. N.A.C.A. T.N. 2250, 1950.
4.	Fraenkel, L.E.	Calculations of the pressure distributions and boundary layer development on a body of revolution. R.A.E. Report Aero. 2482. 1953.
5.	Van Dyke, M.D.	Practical calculation of second order supersonic flow past non-lifting bodies of revolution. N.A.C.A. T.N. 2744 (1952).

No.	Author	Title
6.	Rossow, V.J.	Applicability of the hypersonic similarity rule to pressure distributions which include the effects of rotation for bodies of revolution at zero angle of attack. N.A.C.A. T.N. 2399.
7.	Bolton-Shaw, B.W. Zienkiewicz, H.K.	The rapid accurate prediction of pressure on non-lifting ogival heads of arbitrary shape at supersonic speeds. English Electric Co. Ltd. Rep. No. L.A.t. 034, 1952.
8.	Young, A.D.	Skin friction in the laminar boundary layer in compressible flow. College of Aeronautics Rep. No. 20 (1948) (Also Aero. Quarterly, Vol. 1, Aug. 1949, pp.137-164).

TABLE I

OVERALL SKIN FRICTION COEFFICIENTS - $C_F \times 10^3$

Transition Position	M_o	$R_o = 10^6$	$R_o = 10^7$	$R_o = 10^8$
100%	5.0	1.768	0.559	0.177
"	2.5	1.740	0.550	0.174
"	1.5	1.624	0.514	0.162
$66\frac{2}{3}$%	5.0	1.796	0.652	0.265
"	2.5	2.214	1.013	0.536
"	1.5	2.558	1.320	0.771
0%	5.0	1.825	1.024	0.627
"	2.5	3.095	1.970	1.285
"	1.5	3.977	2.629	1.751

TABLE II

FORM DRAG COEFFICIENTS - $C_{D_p} \times 10^4$

Transition Position	M_o	$R_o = 10^6$	$R_o = 10^7$	$R_o = 10^8$
100%	5.0	1.971	0.601	0.341
'	2.5	0.148	-0.004	-0.003
'	1.5	0.038	0.039	-0.011
$66\frac{2}{3}$%	5.0	1.029	0.207	0.089
'	2.5	-1.201	-1.050	-0.617
'	1.5	-1.471	-1.188	-0.642
0%	5.0	2.769	1.839	1.225
'	2.5	-0.210	-0.350	-0.226
'	1.5	-0.568	-0.307	-0.177

TABLE III

PROFILE DRAG COEFFICIENTS - $C_{D_o} \times 10^3$

Transition Position	M_o	$R_o = 10^6$	$R_o = 10^7$	$R_o = 10^8$
100%	5.0	1.965	0.619	0.211
'	2.5	1.755	0.550	0.174
'	1.5	1.628	0.518	0.161
$66\frac{2}{3}$%	5.0	1.898	0.673	0.274
'	2.5	2.094	0.908	0.474
'	1.5	2.411	1.201	0.707
0%	5.0	2.102	1.208	0.750
'	2.5	3.074	1.935	1.262
'	1.5	3.920	2.598	1.733

APPENDIX

GEOMETRY OF THE BODY CONSIDERED

The forebody is a circular arc ogive and hence with origin at the nose its equation readily follows, viz.-

$$x^2 + r_o^2 - 2x\,L_H + 2r_o\left(\frac{L_H^2}{D} - \frac{D}{4}\right) = 0$$

The radius of the circular ogive is $\left(\frac{L_H^2}{D} + \frac{D}{4}\right)$.

The nose angle θ_S is given by

$$\text{Sin}\,\theta_S = 1 \Big/ \left(\frac{L_H}{D} + \frac{D}{4L_H}\right).$$

For the particular body chosen $L_H = l/3$, $L_H/D = 2.5$.

The centre-body is cylindrical and for the particular body chosen is of the same length as the head i.e. $l/3$.

The boat-tail is formed from a parabolic arc and is such that if its length had been continued to zero cross-sectional radius its length would be $\frac{3}{2}.L_B$, where L_B is its actual length. In consequence the base radius b is equal to $\frac{5}{9}.\frac{D}{2}$. The equation of the boat-tail profile is then

$$r_o = \frac{D}{2}\left\{1 - \frac{4}{9}\,x_B^2\right\},$$

and its length has also been taken to be $l/3$ so that $L_B/D = 2.5$.

FIG. 1.

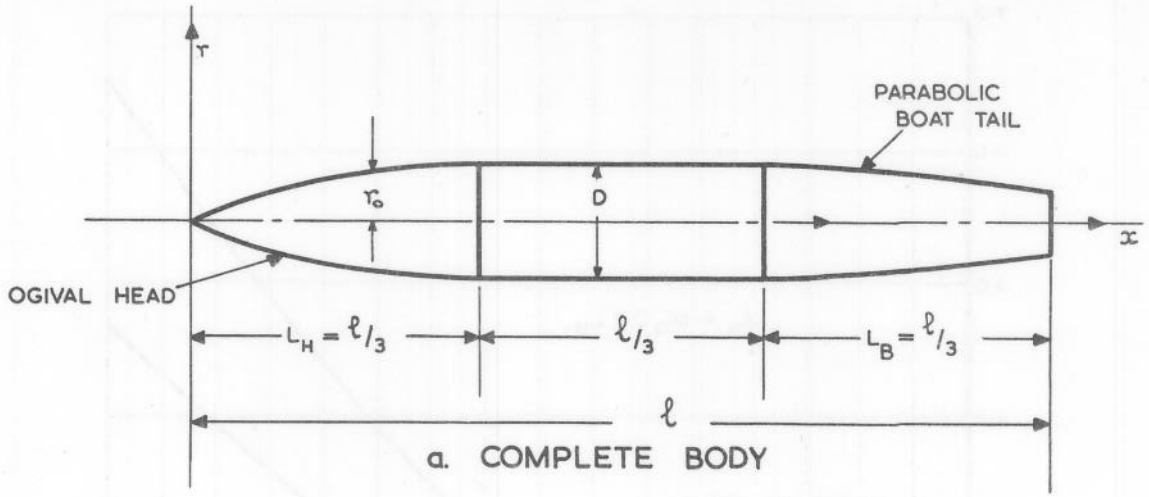

a. COMPLETE BODY

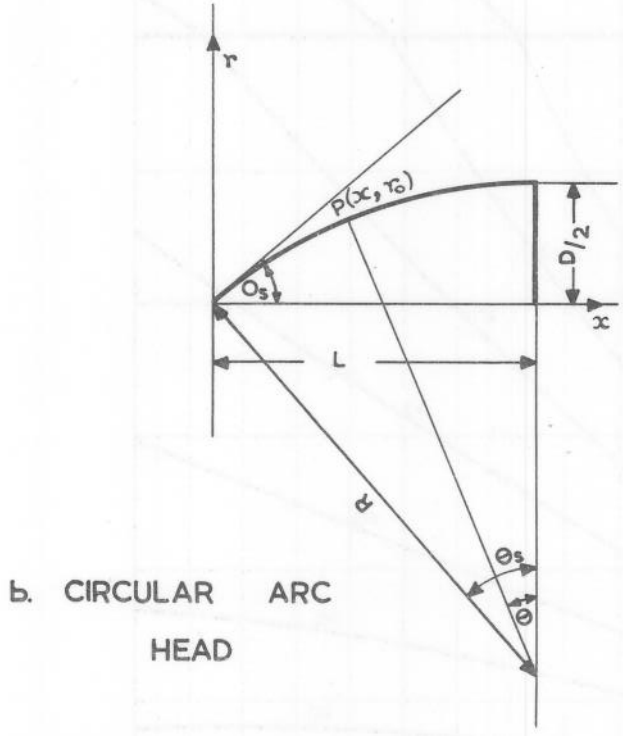

b. CIRCULAR ARC HEAD

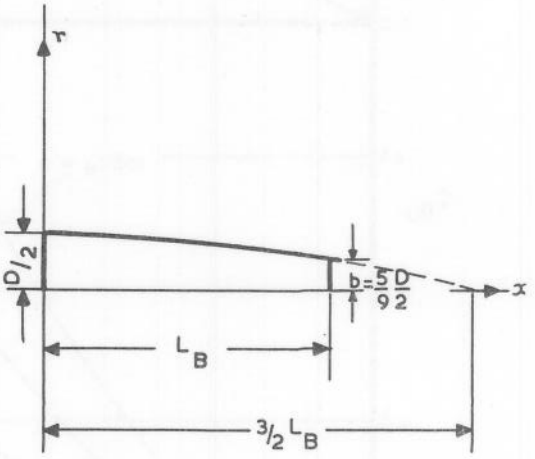

c. PARABOLIC BOAT TAIL

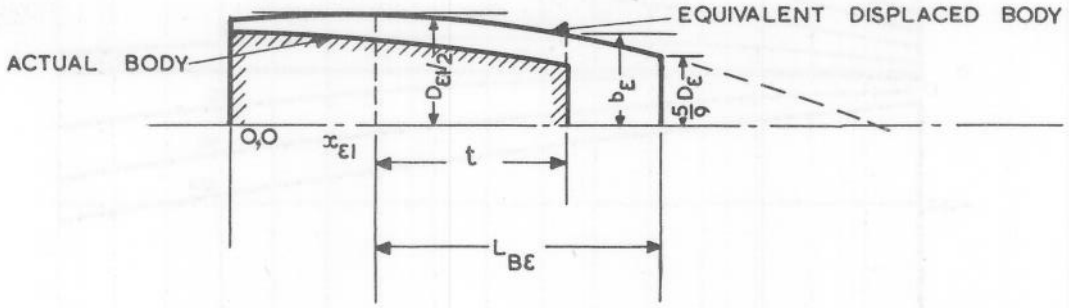

d. EQUIVALENT DISPLACED SHAPE

BODY GEOMETRY (NOT TO SCALE)

FIG. 2.

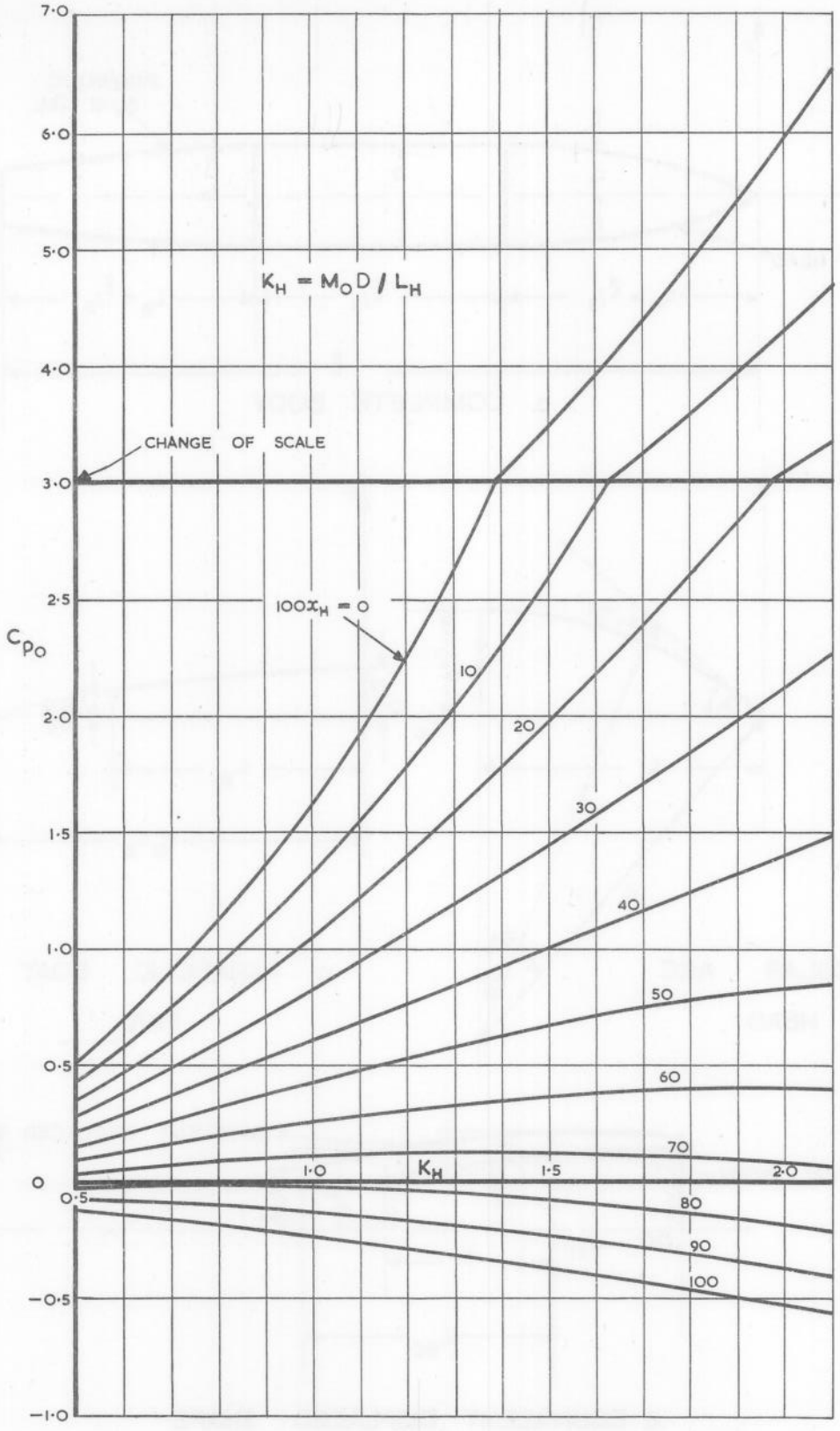

$C_{p_O} \sim K_H$ FOR HEADS

$100x_H$ = PER CENT HEAD LENGTH. (VALUES FOR K > 1·0 OBTAINED FROM REF 3.)

FIG. 3.

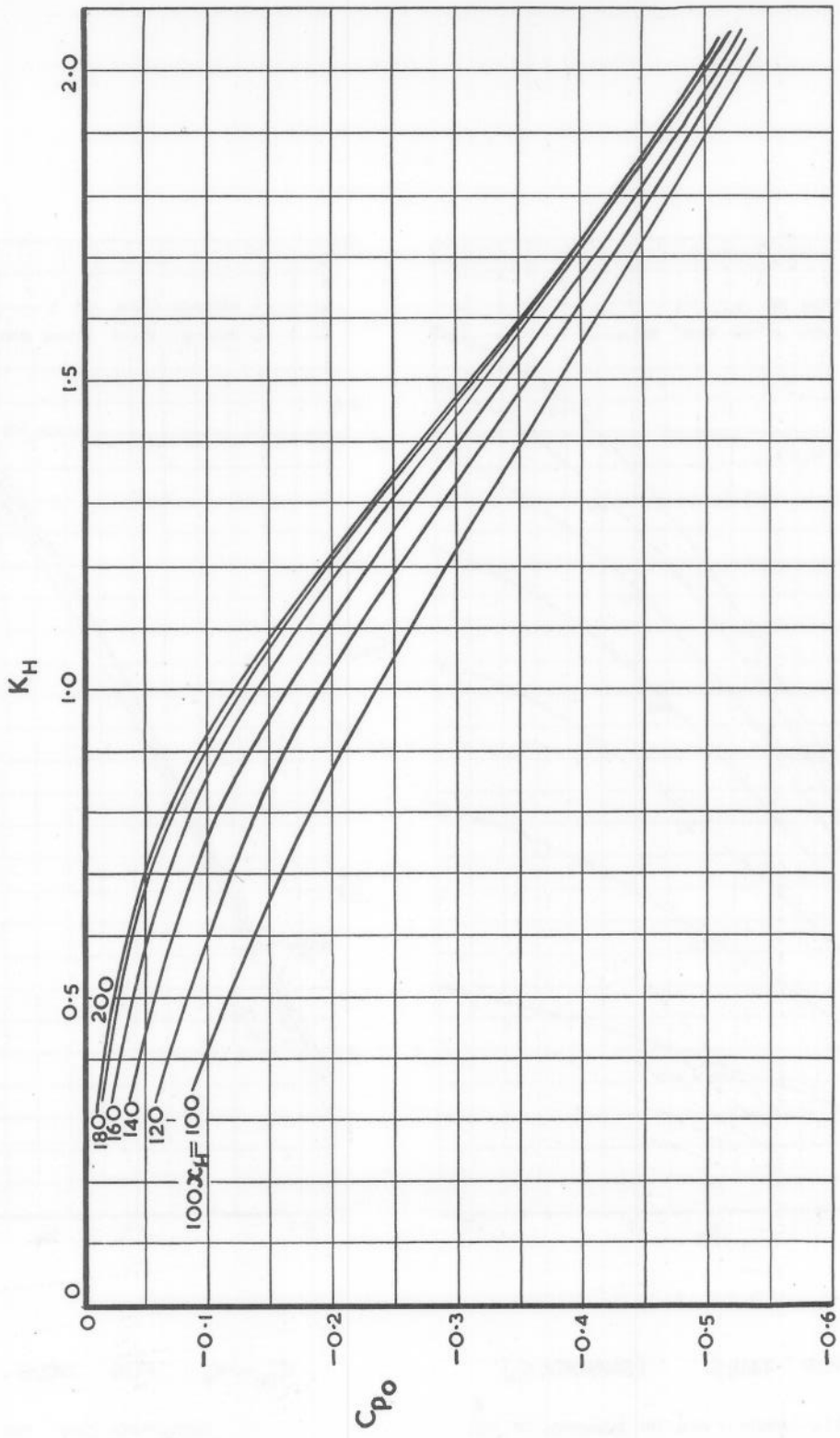

$C_{p_0} \sim K_H$ GRAPH FOR CENTRE SECTION

$100x_H$=PER CENT HEAD LENGTH AFT OF NOSE. (OBTAINED WITH THE HELP OF REF. 3.)

FIGS. 4a. & 4b.

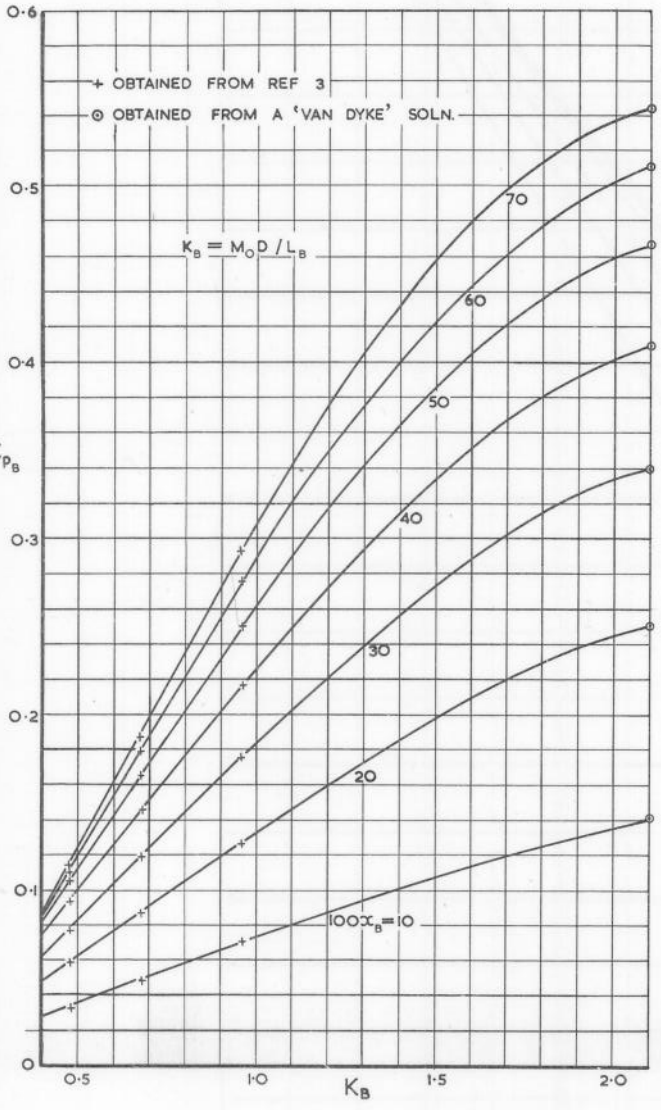

$C_{Pb} \sim K_B$ FOR TAILS. (PARABOLIC.)

$100\mathcal{I}_B$ = PER-CENT TAIL LENGTH. AFT OF BEGINNING OF TAIL.

FIG. 4A.

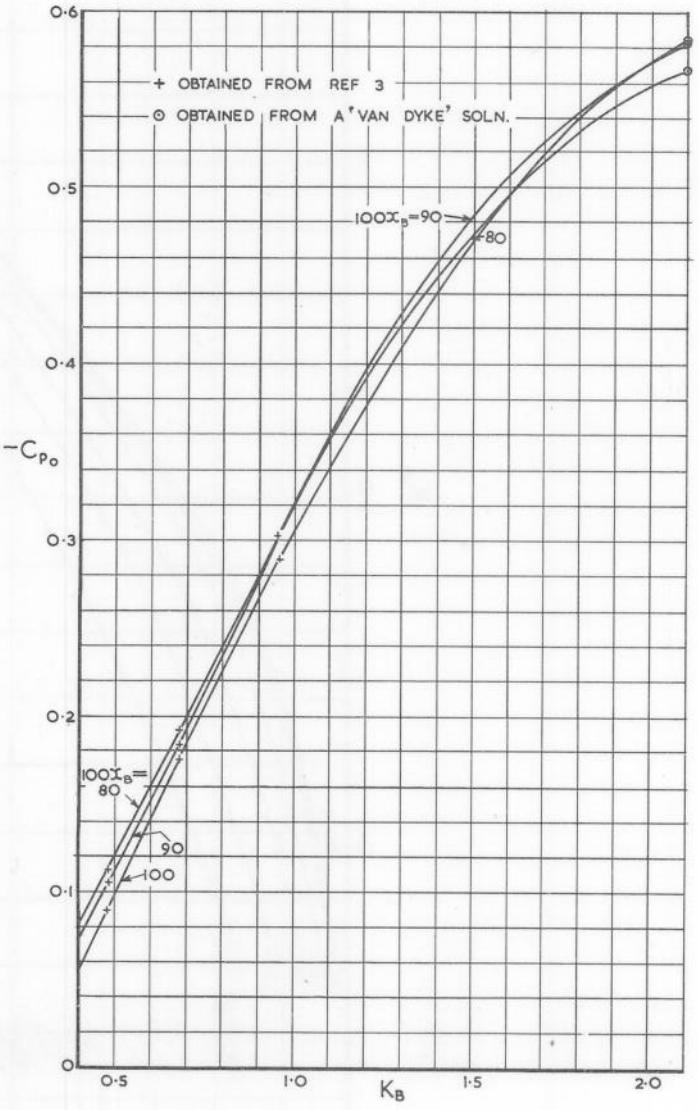

$C_{P_O} \sim K_B$ FOR TAILS (PARABOLIC.)

$100\mathcal{I}_B$ = PER CENT TAIL LENGTH.

FIG. 4B.

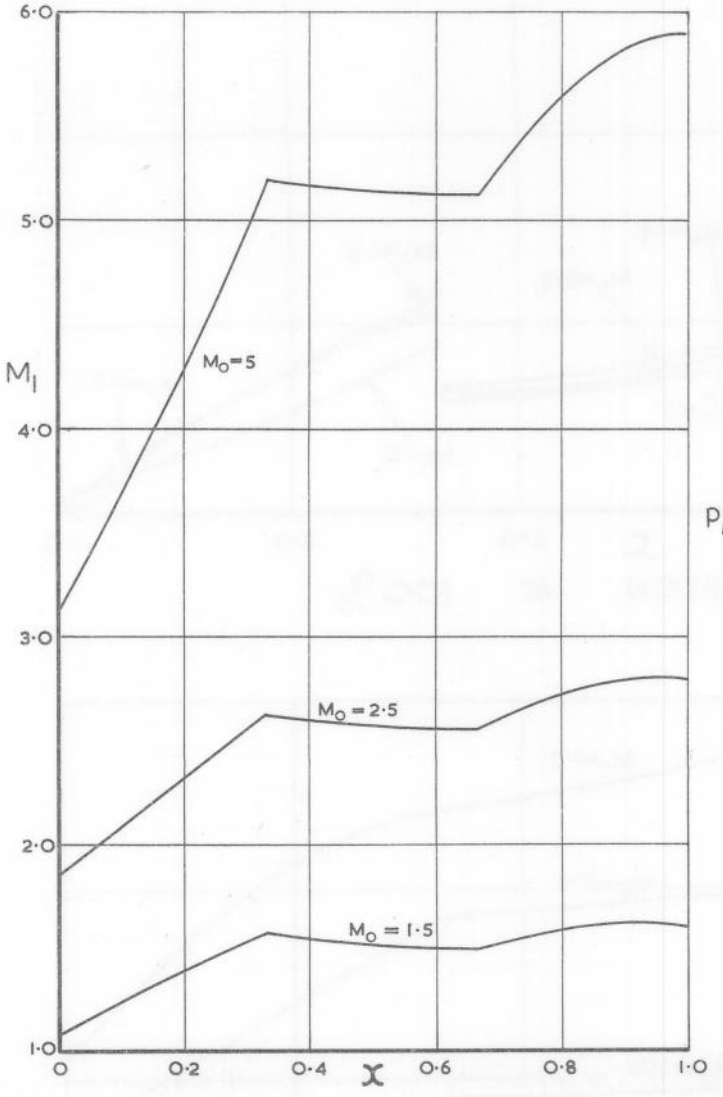

DISTRIBUTION OF M_1 OVER BODY
$\ell/D = 7·5$

FIG. 5.

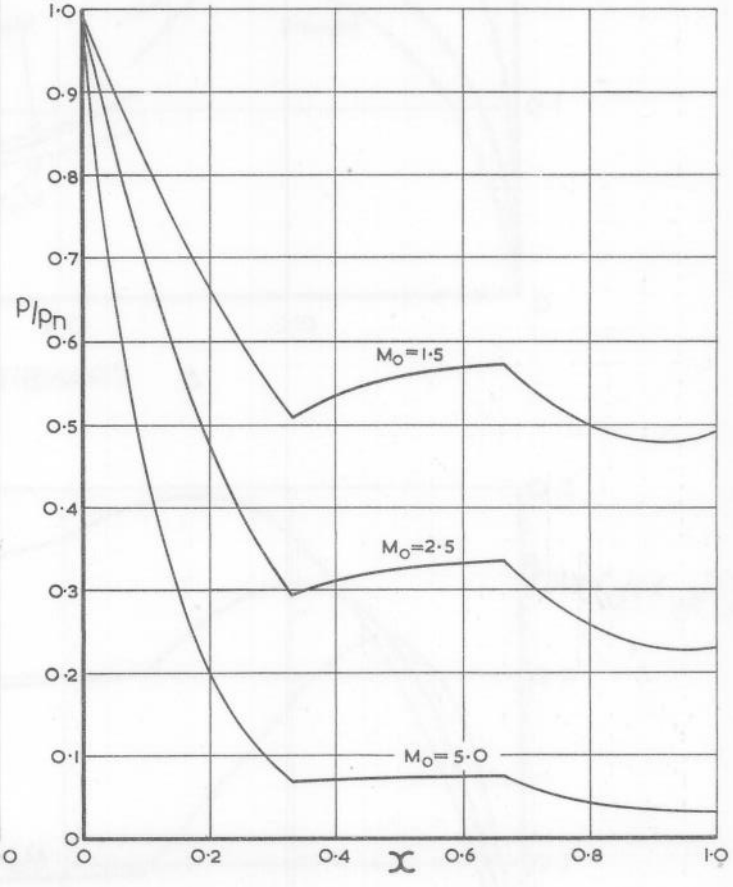

$p/p_n \sim x$ FOR $\ell/D=7·5$

FIG. 6.

FIG. 7.

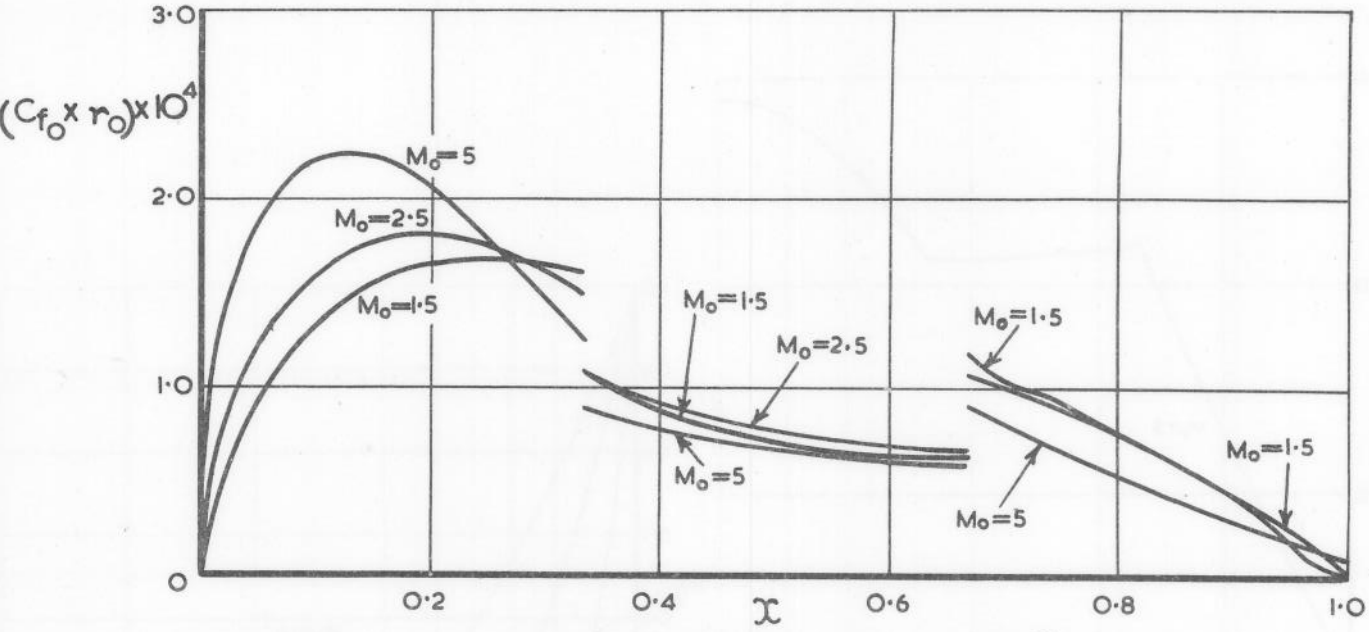

a. TRANSITION AT 100 %

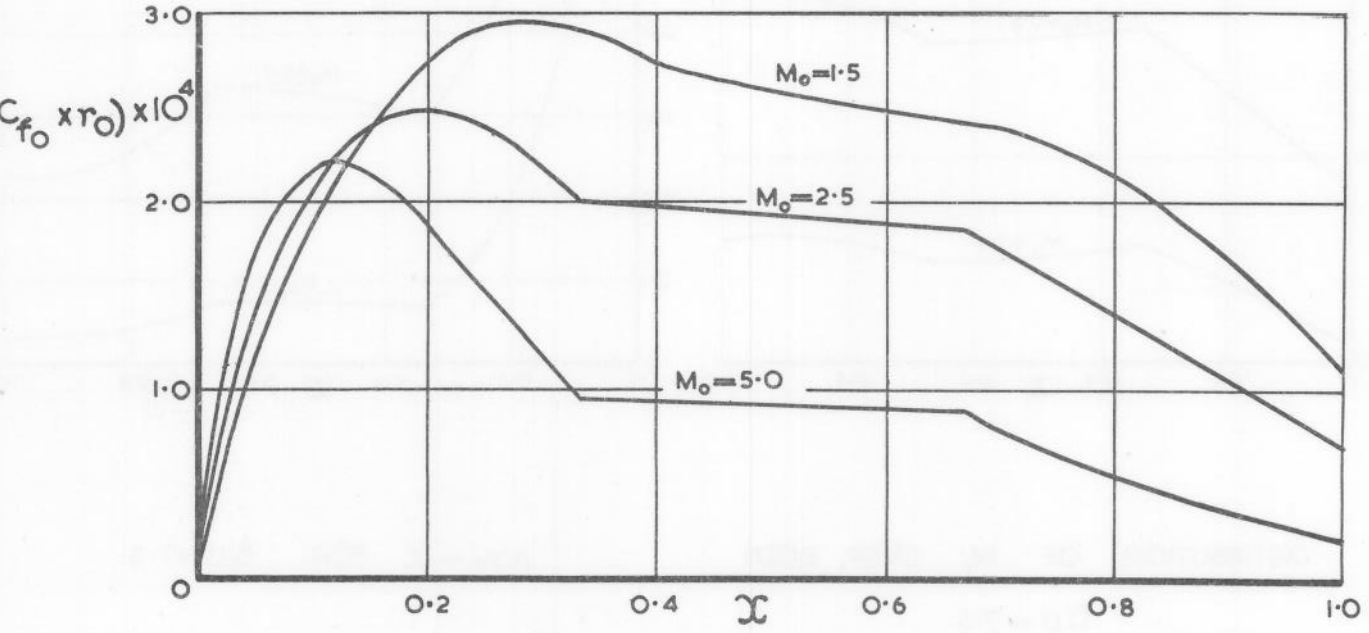

b. TRANSITION AT 0 %

$C_{f_o} \times r_o$ DISTRIBUTIONS AT $R_o = 10^6$

$\ell / D = 7·5$

FIG. 8.

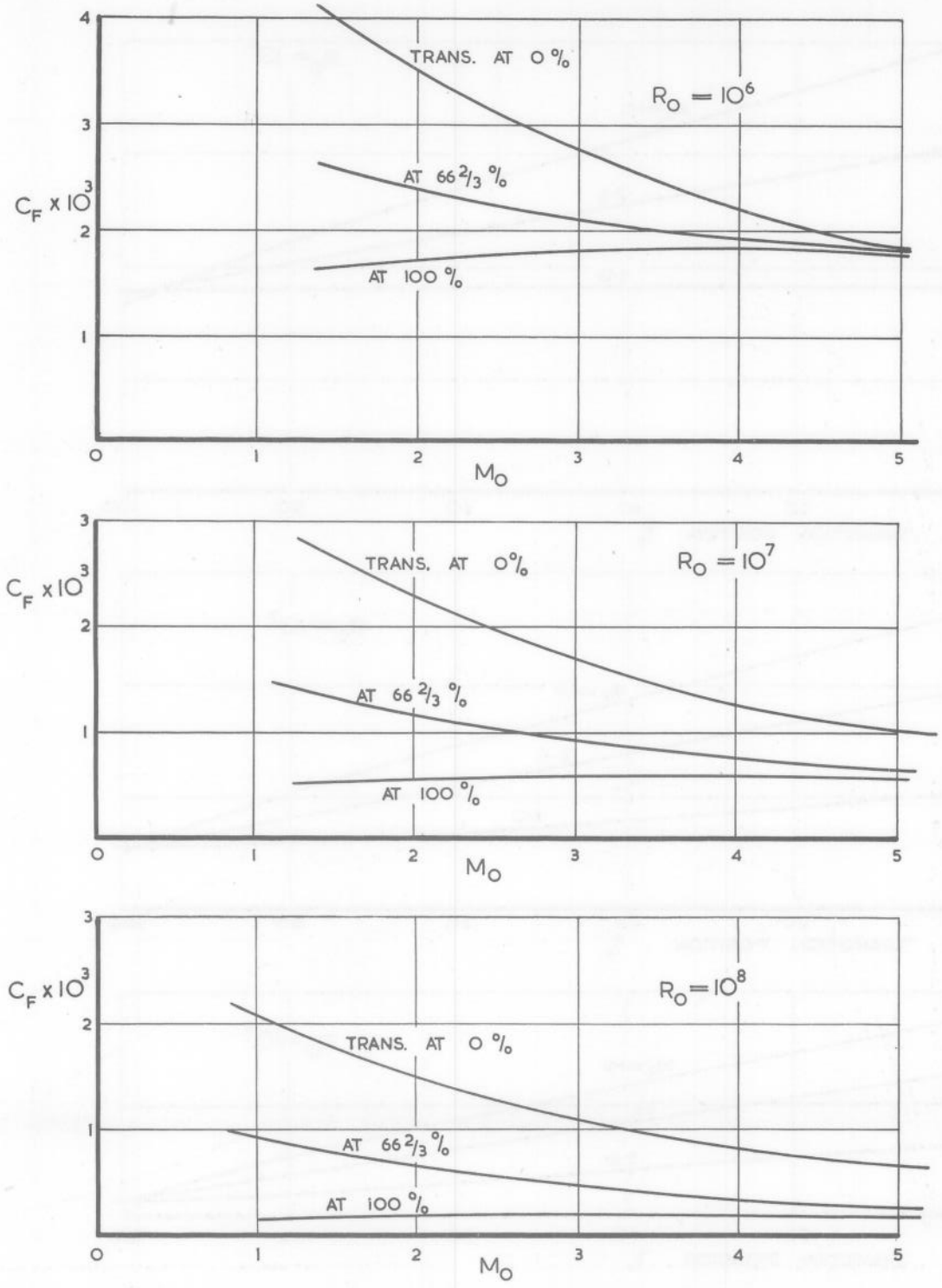

VARIATION OF TOTAL SKIN FRICTION (C_F) COEFFICIENT WITH MACH No.

FIG. 9.

COLLEGE OF AERONAUTICS
REPORT No. 81.

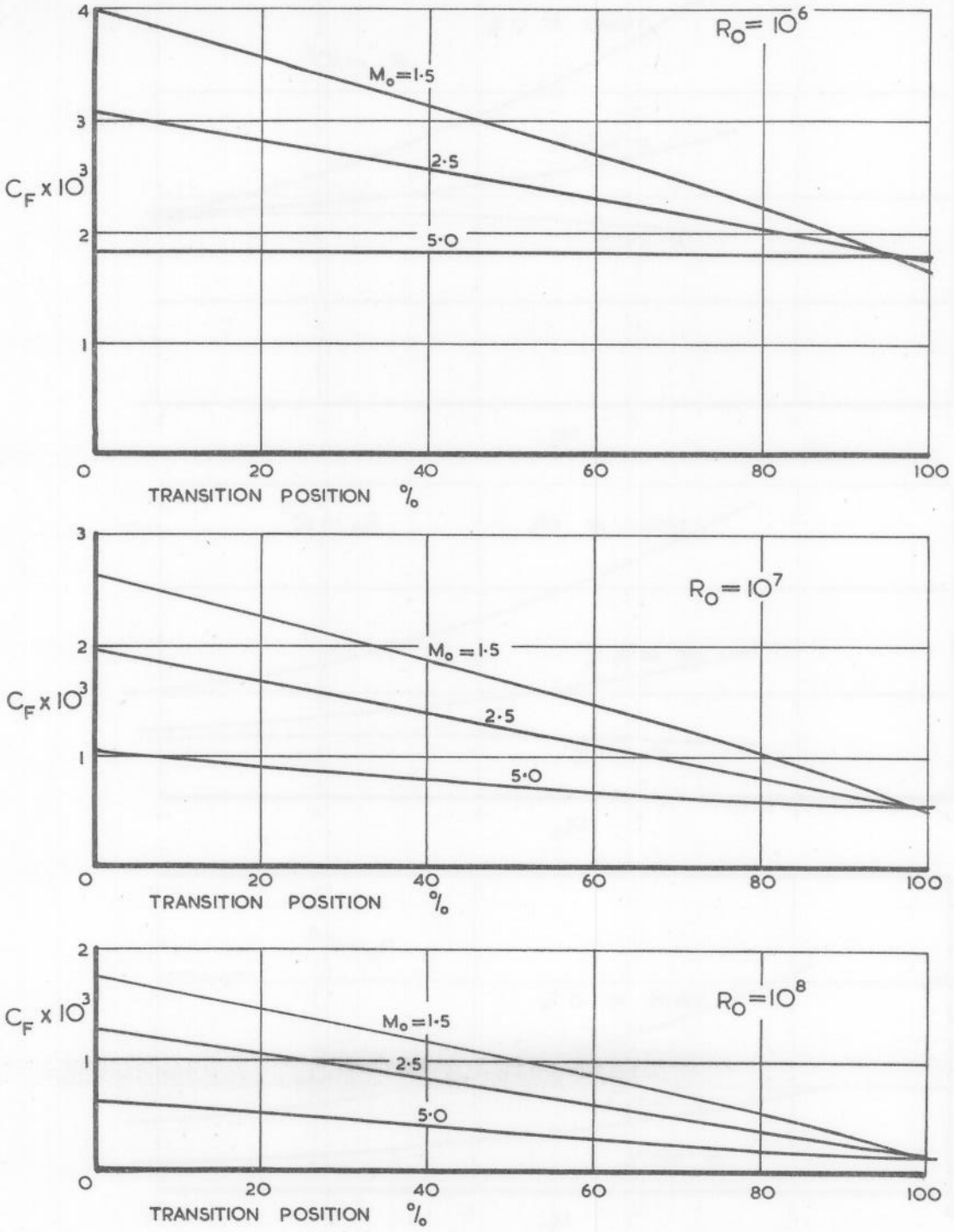

VARIATION OF TOTAL SKIN FRICTION COEFFICIENT (C_F) WITH TRANSITION POSITION $\ell/D = 7.5$

FIG. 10.

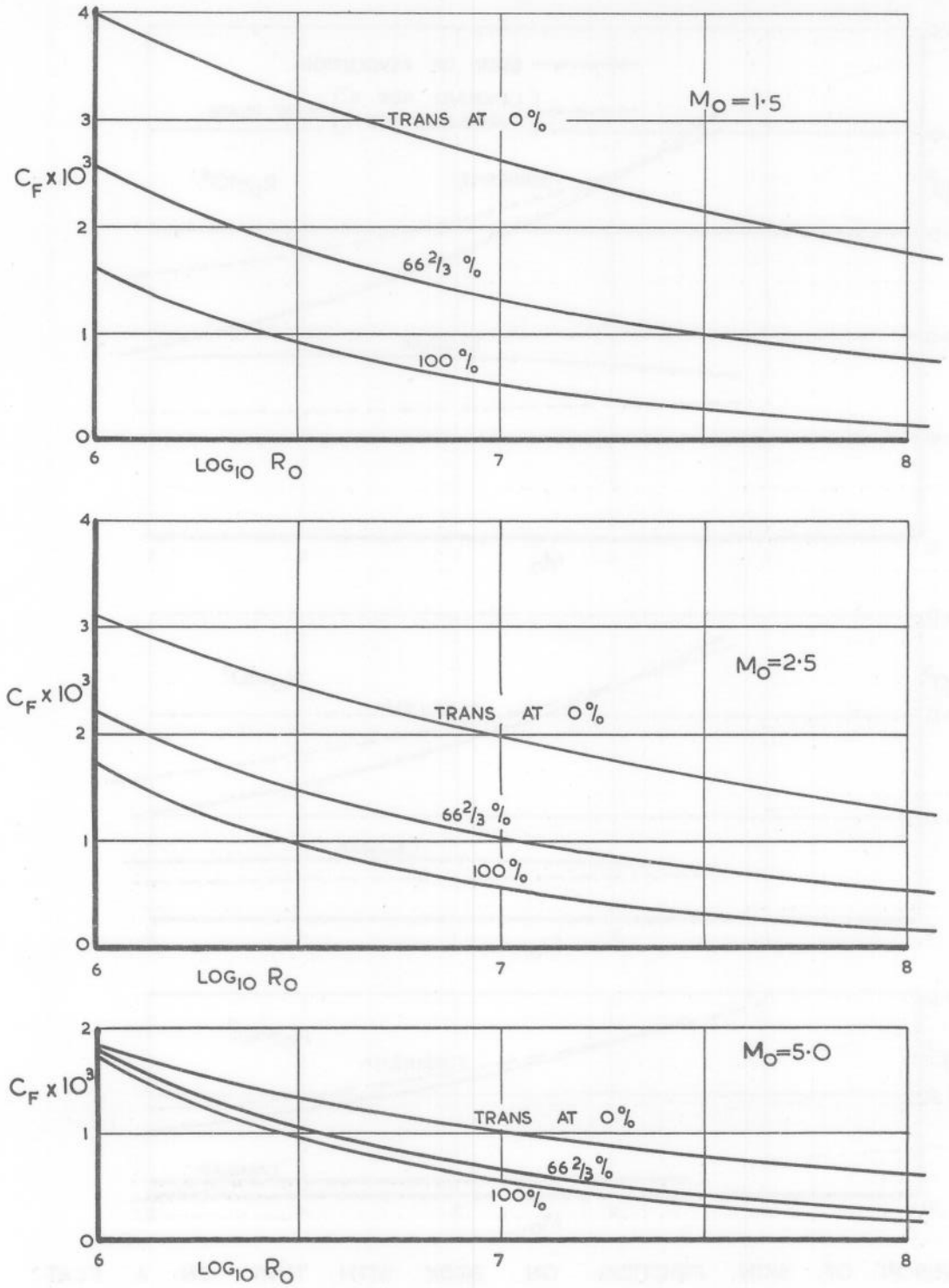

VARIATION OF TOTAL SKIN FRICTION COEFFICIENT (C_F) WITH REYNOLDS NUMBER (R_O)

$\ell/D = 7{\cdot}5$

FIG. 11.

COLLEGE OF AERONAUTICS
REPORT No. 81.

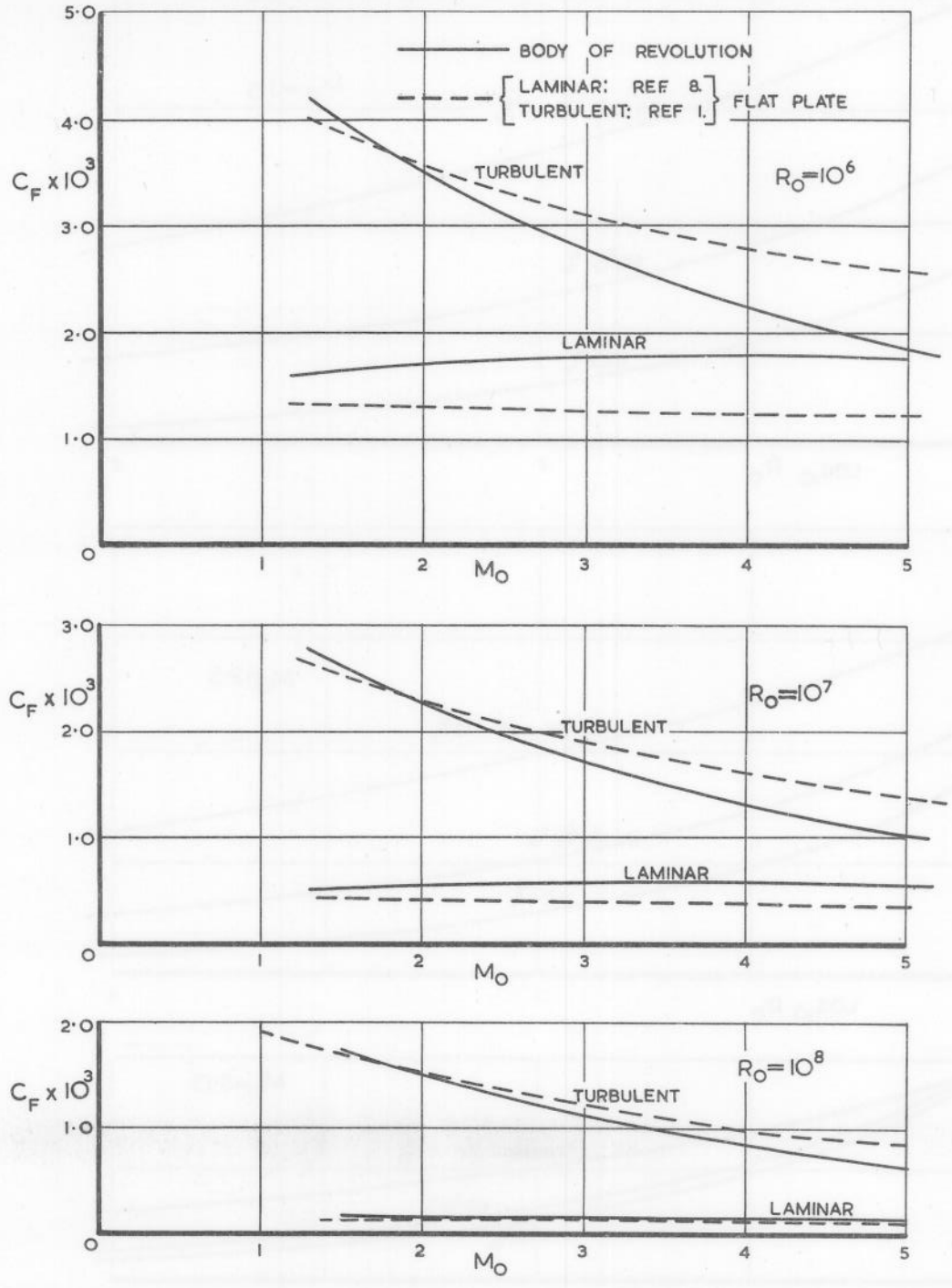

COMPARISON OF SKIN FRICTION ON BODY WITH THAT ON A FLAT PLATE OF THE SAME SURFACE AREA.

FIG. 12.

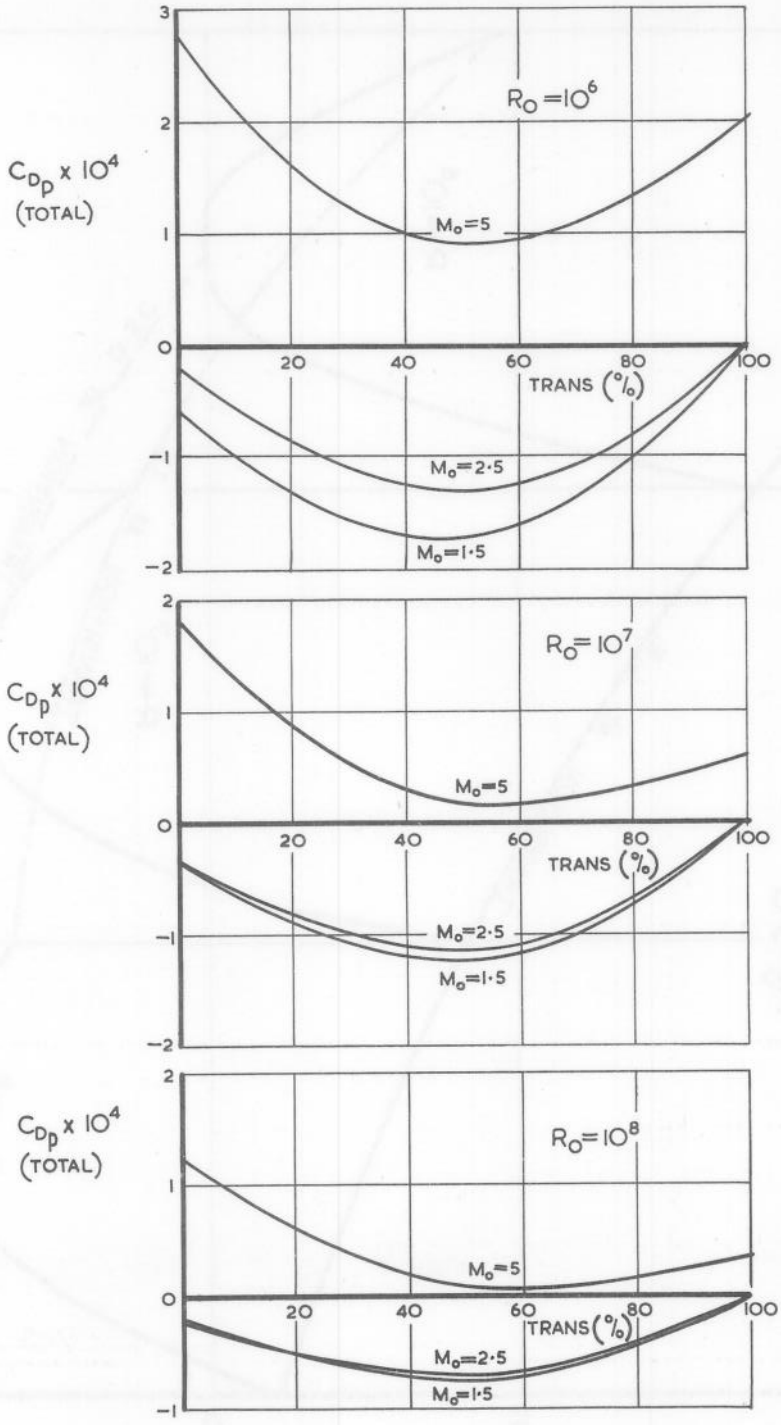

FORM DRAG COEFFICIENT AS A FUNCTION OF TRANSITION POSITION.

$\ell/D = 7{\cdot}5$

FIG. 13.

COLLEGE OF AERONAUTICS

REPORT No. 81.

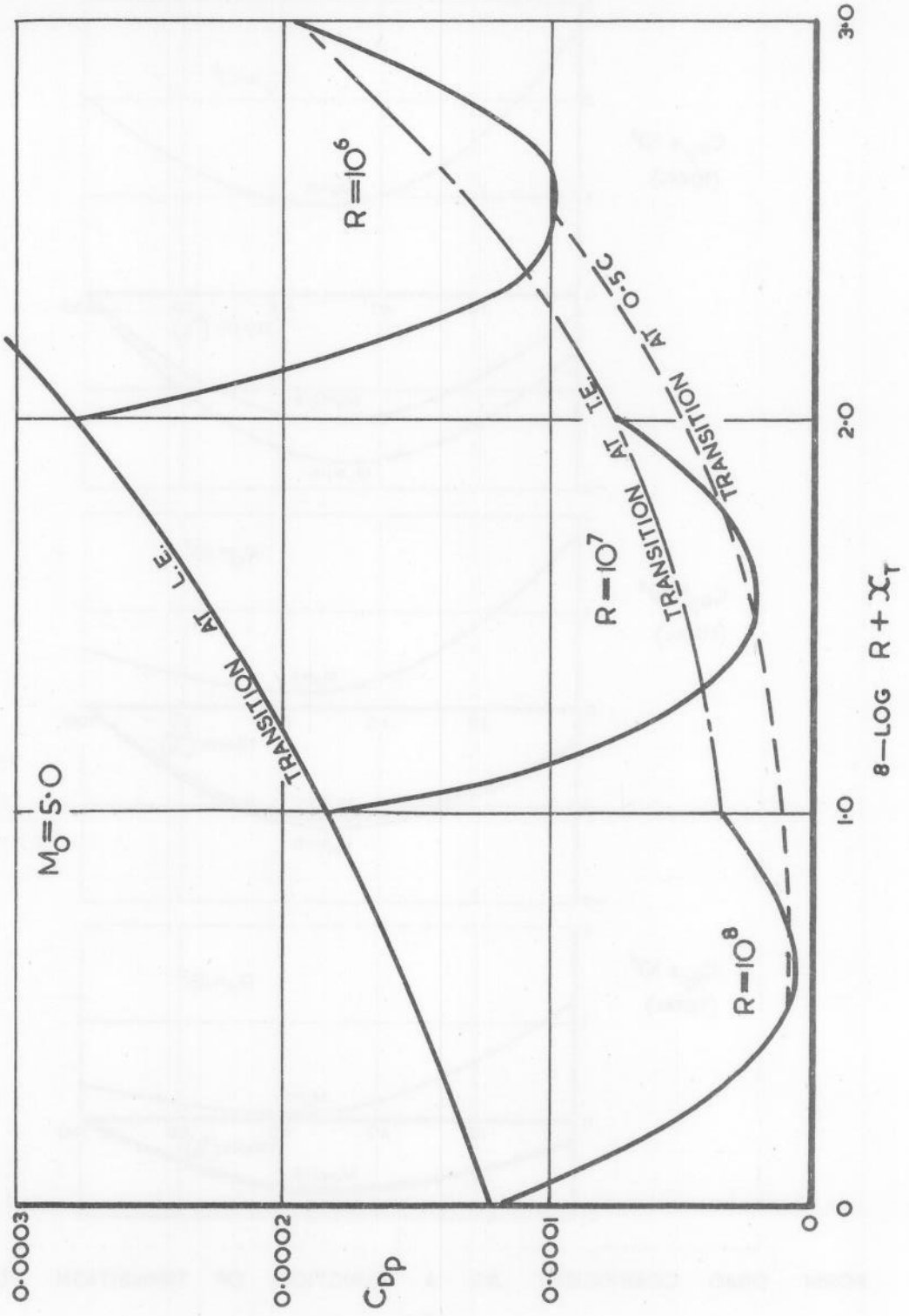

FORM DRAG COEFFICIENT AS A FUNCTION OF TRANSITION POSITION AND R.N. $\ell/D = 7 \cdot 5$

FIG. 14.

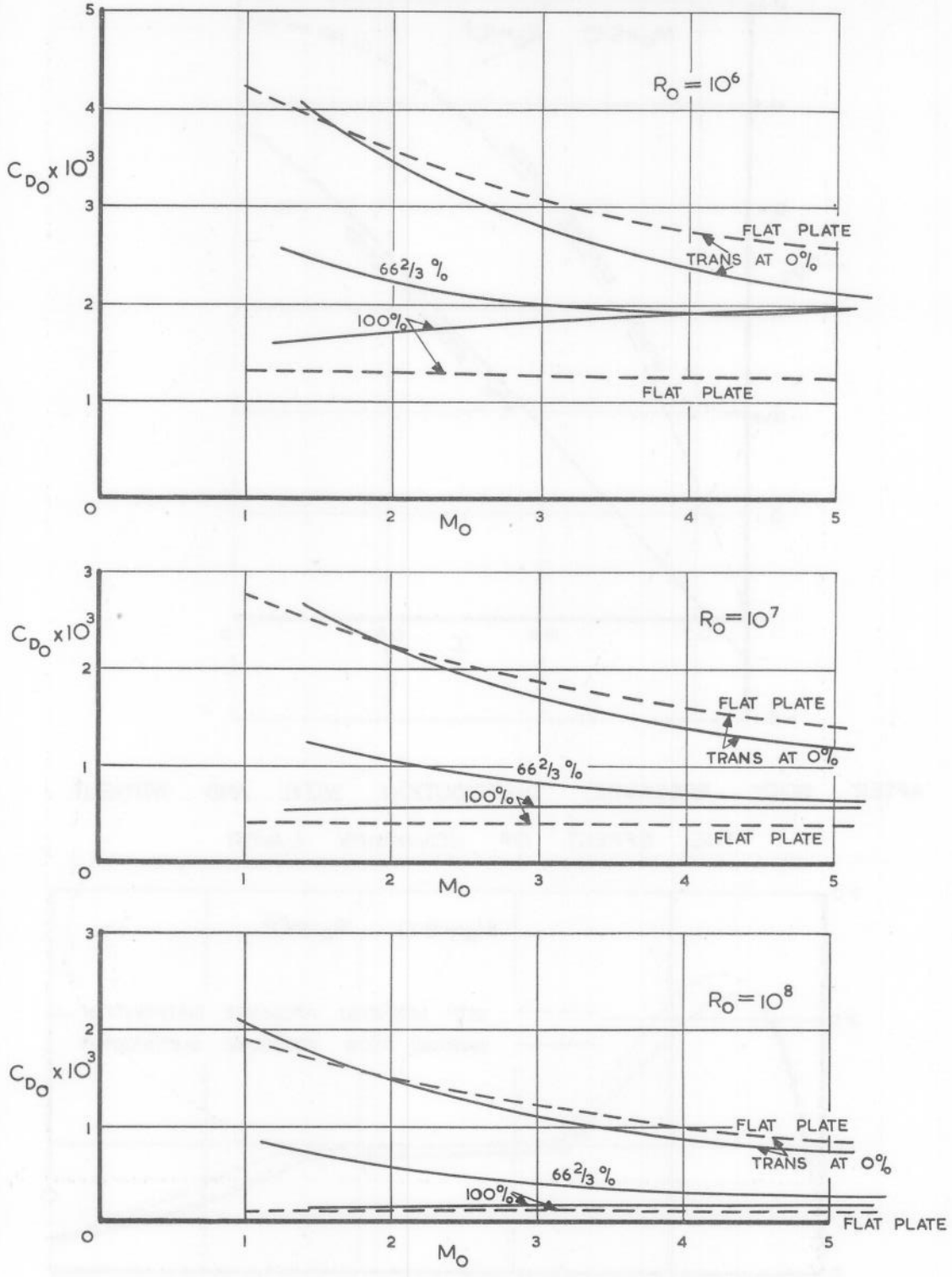

VARIATION OF PROFILE DRAG WITH MACH NUMBER. $l/D = 7{\cdot}5$

FIG. 15.

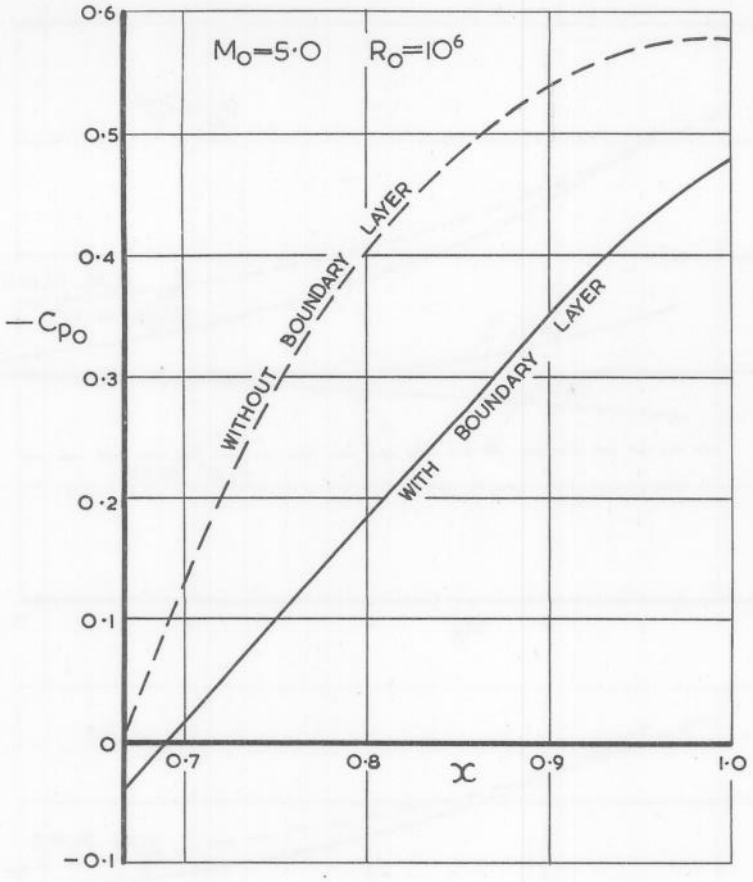

a. AFTER BODY PRESSURE DISTRIBUTION WITH AND WITHOUT THE EFFECT OF BOUNDARY LAYER

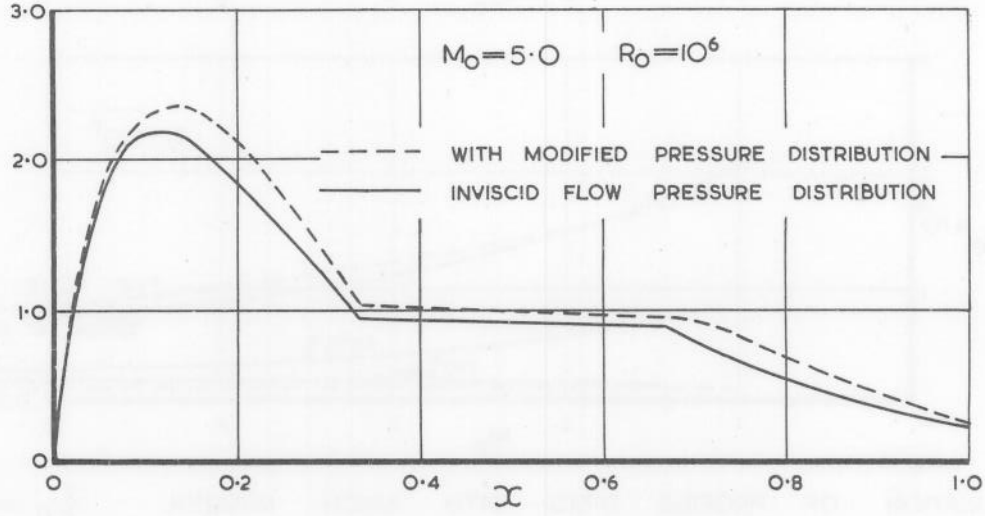

b. THE EFFECT OF THE RECALCULATED PRESSURE DISTRIBUTION (DUE TO B. L. DISPLACEMENT EFFECT) ON LOCAL SKIN FRICTION